A Near-Threshold Shape Resonance in the Valence-Shell Photoabsorption of Linear Alkynes

U. Jacovella, U. Holland, S. Boyé-Péronne, Bérenger Gans, N. de Oliveira, K. Ito, D. Joyeux, L. E. Archer, R. Lucchese, Hong Xu, et al.

Title

A Near-Threshold Shape Resonance in the Valence-Shell Photoabsorption of Linear Alkynes

Journal

The Journal of Physical Chemistry A, 119(50)

ISSN

1089-5639

Authors

Jacovella, U

Holland, DMP

Boyé-Péronne, S

et al.

Publication Date

2015-12-17

DOI

10.1021/acs.jpca.5b06949

Peer reviewed

A NEAR-THRESHOLD SHAPE RESONANCE IN THE VALENCE-SHELL PHOTOABSORPTION OF LINEAR ALKYNES

U. Jacovella,[a] D. M. P. Holland,[b] S. Boyé-Péronne,[c] Bérenger Gans,[c] N. de Oliveira,[d] K. Ito,[d] D. Joyeux,[d] L. E. Archer,[d] R. R. Lucchese,[e] Hong Xu,[f] and S. T. Pratt[f]

[a]Laboratorium für Physikalische Chemie, ETH Zürich, 8093 Zürich, Switzerland

[b]STFC, Daresbury Laboratory, Daresbury, Warrington, Cheshire WA4 4AD, UK

[c]Institut des Sciences Moléculaires d'Orsay , UMR 8214, CNRS & Univ. Paris-Sud, F-91405 Orsay, France

[d]Synchrotron Soleil, L'Orme des Merisiers, F-91192 Gif-sur-Yvette, France

[e]Department of Chemistry, Texas A&M University, College Station, Texas 77843 USA

[f]Argonne National Laboratory, Argonne, IL 60439 USA

ABSTRACT

The room-temperature photoabsorption spectra of a number of linear alkynes with internal triple bonds (e.g., 2-butyne, 2-pentyne, and 2- and 3-hexyne) show similar resonances just above the lowest ionization threshold of the neutral molecules. These features result in a substantial enhancement of the photoabsorption cross sections relative to the cross sections of alkynes with terminal triple bonds (e.g., propyne, 1-butyne, 1-pentyne, …). Based on earlier work on 2-butyne [H. Xu et al., J. Chem. Phys. **136**, 154303 (2012)], these features are assigned to excitation from the neutral HOMO to a shape resonance with g (l = 4) character, and approximate π symmetry. This generic behavior results from the similarity of the HOMOs in all internal alkynes, as well as the similarity of the corresponding gπ virtual orbital in the continuum. Theoretical calculations of the absorption spectrum above the ionization threshold show a strong l = 4 contribution for the 2- and 3-alkynes, but no such contribution for the 1-alkynes. These calculations thus confirm the qualitative arguments for the importance of the l = 4 continuum near threshold for internal alkynes, which should also apply to other linear internal alkynes and alkynyl radicals. However, the calculations for 2-pentyne and 2- and 3-hexyne do not show evidence for strong l = 4 shape resonance enhancement near threshold, and the possible reasons for this are discussed.

I. INTRODUCTION

Shape resonances in molecular photoionization can have a dramatic effect on cross sections, final-state branching ratios, and photoelectron angular distributions.[1-4] These resonances are caused by the temporary trapping of photoelectrons with high angular momentum, *l*, by the centrifugal barrier in the electron-ion potential. These resonances are often also associated with virtual valence orbitals in the continuum. At threshold, the amplitude of higher-*l* wavefunctions at short range is typically quite small, and the shape resonances are generally found to occur at somewhat higher energies, where the electron penetrates the centrifugal barrier and the build up of amplitude at short range can occur.[1-4] However, in larger molecules, the molecular frame can support partial waves of higher *l*, and the resonances may occur at energies much closer to threshold. For example, Staniforth *et al*.[5,6] have recently described a generic shape resonance of π symmetry that is observed in the two-photon excitation of ortho-, meta-, and para-difluorobenzene just above the first ionization threshold. As another example, the photoabsorption and photoionization cross sections for 2-butyne show an intense broad feature just above the first ionization threshold that has been assigned to excitation from the highest occupied molecular orbital (HOMO) of the neutral ground state into an $l = 4$, gπ shape resonance.[7] This example is interesting because the high-*l* states are directly accessed from the ground state of the neutral molecule. In the present paper, the observations for 2-butyne are extended to the pentynes and hexynes to investigate the generality of this behavior.

To illustrate the effects of such shape resonances, Figure 1 shows the low-resolution photoionization cross sections for acetylene, propyne, and 1- and 2-butyne from the work of Cool and co-workers.[8-10] Here, the cross sections for acetylene, propyne, and 1-butyne show similar behaviors and magnitudes, while the cross section for 2-butyne is dramatically enhanced. In a previous study of the threshold shape resonance in 2-butyne,[7] not only was the character of the HOMO used to rationalize this enhancement, but, as described in more detail below, the very different character of the HOMOs in acetylene, propyne, and 1-butyne provided a rationalization

for the absence of transitions to gπ shape resonances in the photoabsorption spectrum of these species. The HOMOs in acetylene, propyne, and 2-butyne are doubly degenerate orbitals centered on the C≡C triple bond;[7,11] these orbitals are split in the larger alkynes (e.g., 1-butyne, 1- and 2-pentyne, and 1-, 2-, and 3-hexyne) owing to the loss of quasi-cylindrical symmetry. The HOMO and HOMO-1 of 1-butyne and the HOMO of 2-butyne are shown in Figure 2, and the corresponding orbitals for 1-, and 2- pentyne, and 1-, 2-, and 3-hexyne are shown in Figures 3a and 3b. The geometries of the molecules were determined using the MP2 method with a 6-311++G(2df,p) basis set, as implemented in Gaussian 09.[12] The orbitals and orbital energies shown in Figures 2 and 3 correspond to the canonical Hartree-Fock orbitals obtained with the same basis set. Although the HOMO and HOMO-1 of some of these molecules are split, the calculated splittings between the HOMO and HOMO-1 are small, ranging from 0.010 to 0.038 eV with this theoretical method. Furthermore, as seen in Figures 2 and 3, the electron density of both the HOMO and HOMO-1 show similar distributions centered on the C≡C triple bond.

In the earlier work of Reference 7, the similarity of the 2-butyne HOMO to a "stretched" fπ atomic orbital was noted, and the atomic selection rule $l \rightarrow l \pm 1$, with $l \rightarrow l + 1$ significantly stronger,[13,14] was used to rationalize the observed strength of the transition to the gπ shape resonance just above threshold. In contrast, a single-center expansion of the HOMO/HOMO-1 of 1-butyne suggests that it arises from a stretched linear combination of pπ and dπ orbitals that interfere constructively across the triple bond, and destructively across the ethyl group. In an atomic picture, this HOMO would lead to excitation involving p → s, d and d → p, f transitions, but little excitation into g (l = 4) Rydberg states or continua. Figures 2 and 3 suggest that the same arguments should extend to the larger alkyne molecules. In particular, based on the structure of the HOMO/HOMO-1 orbitals, the terminal alkynes, 1-pentyne and 1-hexyne, are expected to behave like 1-butyne and propyne, with no shape resonance enhancement in the single-photon absorption spectrum just above threshold, while the internal alkynes, 2-pentyne and 2- and 3-hexyne, are expected to show strong transitions to the analogous gπ shape

resonances in these molecules.

In this paper, we present new room-temperature photoabsorption measurements of 1- and 2-pentyne, and 1-, 2-, and 3-hexyne in the region from the first Rydberg excitation to a photon energy approximately 1 - 2 eV above the ionization threshold (7.4 eV to 11.2 eV). We were unable to find any previous vacuum ultraviolet photoabsorption spectra for the pentynes or hexynes in this energy region. While the spectra show considerable bound state structure, here we focus on the behavior of the cross section just above threshold, in the region where the $g\pi$ shape resonance is expected. We also present theoretical calculations of the photoabsorption cross sections above the lowest ionization threshold. To a large degree, the experimental spectra confirm expectations about the behavior of this shape resonance in terminal and internal alkynes. The results are discussed in terms of their implications for other systems, as well as their implications for the bound state spectra of these molecules.

II. EXPERIMENT

The experiments were performed at the Synchrotron SOLEIL on the Vacuum Ultraviolet-Fourier Transform Spectrometer (VUV-FTS) branch of the DESIRS beamline, which has been described in detail previously.[15-17] Here we present only the details specific to the present experiment. The spectra of 1- and 2-butyne, 1- and 2-pentyne, and 1-, 2-, and 3-hexyne were recorded by using two different sample cells: a windowed cell for calibrating the absolute photoabsorption cross sections; and a flowing cell for recording high-resolution, room-temperature spectra. The FTS calibration process and the potential sources of error in cross sections are described in detail in a forthcoming publication.[18] Experimental uncertainties in the cross-section determinations using the flowing cell are estimated to be about ±10% in the spectral region above the ionization threshold, with the primary contribution coming from the calibration of the column density. 1-butyne (ABCR GmbH & Co., 98% purity) is a gas at room temperature and was used directly

from the cylinder. All of the other samples (ABCR GmbH & Co., 98-99% purity) are high-vapor pressure liquids at room temperature, and the gas above the liquid was used.

Individual sections of the full spectra were recorded at several different undulator settings across the energy range of interest. Each of these sections was recorded by using the full bandwidth of the undulator after the synchrotron light had passed through a harmonic-removing gas filter. The individual sections were then spliced together, and calibrated by using impurity lines in the gas filter. The Fourier-transform data were recorded with sufficient resolution to provide 0.9 meV resolution in the transformed spectra. However, because the features in the continuum are broad, the Fourier transforms in this region were computed with 1.7 meV resolution to improve the signal to noise ratio.

III. RESULTS AND DISCUSSION

A. Experimental Photoabsorption Spectra

Figure 4 shows the absorption spectra of 1- and 2-butyne recorded with the FTS and plotted with the same *y* scale. The bound-state structure in these spectra has been discussed previously,[19] and here we focus on the structure of the ionization continua. The ionization energies of 1- and 2-butyne are 10.178 ± 0.005 eV and 9.5611 ± 0.0006 eV, respectively.[20-22] As was discussed previously, the absorption cross section for 1-butyne is in good agreement with earlier measurements.[23] The cross section above 10.6 eV remains flat up to at least 11.8 eV, the limit of the earlier data.[23] The cross section for 2-butyne agrees well with previous measurements[24] below the ionization threshold, but at higher energy the present cross section is smaller. For example, at the peak of the shape resonance the present 2-butyne cross section is about 30% smaller than in the previous study by Palmer and Walker.[24] Nevertheless, Figure 4 clearly shows the strong enhancement of the cross section by the shape resonance in 2-butyne, in contrast to the relatively flat continuum in 1-butyne.

At the peak of the 2-butyne resonance (10.415 eV), the present absorption cross section is ~36% bigger than the 1-butyne cross section at the same energy. Note, however, that in the ionization spectra of Figure 1 (as opposed to the absorption spectra of Figure 4), the ionization cross section of 2-butyne is much larger than that of 1-butyne throughout the energy range of the figure. This large difference is due to three factors. First, the overall magnitude of the photoabsorption cross section is strongly enhanced by the shape resonance in 2-butyne. However, the impact of this increase on the photoionization cross section depends on the quantum yield for ionization following excitation into the shape resonance. The second factor is that the ionization quantum yield for 1-butyne at this energy is relatively small because it is just above the ionization threshold and, at least below ~10.8 eV, the full Franck-Condon envelope of the ionic ground state is not energetically accessible. Finally, as discussed previously,[7] the quantum yield for ionization following excitation into the shape resonance of 2-butyne is nearly unity. This value can be inferred because, as reported previously,[17] the enhancements in the photoabsorption and photoionization cross sections of 2-butyne track each other pretty much 1:1 across the shape resonance. In contrast, at energies above the resonance (~11.16 eV), the quantum yield for ionization in 2-butyne is only ~60% to 80%, depending on whether photoabsorption data of Palmer and Walker[24] or the present study are used. For comparison, at 10.54 eV, the quantum yield for ionization of 1-butyne is ~35% using the present data and the photoionization cross section of Wang *et al*.[10] Between 10.66 eV and 11.41 eV, the 1-butyne quantum yield extracted from the data of Nakayama and Watanabe[23] is somewhat larger, ranging between ~55% and 70%. Thus, the shape resonance in 2-butyne not only increases the photoabsorption cross section, but also increases the effective quantum yield for ionization. The high ionization yield for excitation into the shape resonance likely reflects its very large width (i.e., short lifetime), which suggests that ionization occurs much more rapidly than other competing radiationless transitions and dissociation.

Figures 5 and 6 show the photoabsorption spectra of 1- and 2 pentyne, and 1-, 2, and 3-hexyne, respectively, and Table I summarizes the corresponding ionization energies and resonance positions. A figure showing all of these spectra together, along with those of propyne and 1- and 2-butyne, is included in the Supplemental Material.[25] As expected from the discussion above, the spectra for 1-pentyne and 1-hexyne show no evidence for a shape resonance near the ionization thresholds, while the spectra for the internal alkynes all show a strong broad resonance just above the first ionization limit. The similarity of the resonances suggests that they have a common source and, given the similarities among the HOMOs and HOMO-1s of all of these molecules (see Figures 3a and 3b), it is likely that the resonances all have $l = 4$, gπ character. The resonance in 3-hexyne is somewhat more pronounced than that in 2-pentyne or 2-hexyne, which may reflect the more symmetric character of the former molecule.

Yang and Hansen[26] have recently determined the absolute photoionization cross sections for 1- and 2-pentyne, while the corresponding cross sections for the hexynes are currently unavailable. The behavior of the pentyne cross sections is similar to that of the butyne cross sections. In particular, the 2-pentyne photoionization cross section tracks the photoabsorption cross section from just above threshold to ~11.5 eV, indicating an ionization quantum yield of essentially unity; the 1-pentyne photoionization cross section is considerably smaller than the photoabsorption cross section in the same region, with an ionization quantum yield of ~0.5. These observations are consistent with the high expected ionization quantum yield for the shape resonance in 2-pentyne, and provide strong support for the arguments presented here.

The peak of the shape resonance in 2-butyne lies approximately 0.85 eV above the ionization threshold (see Figure 4). Because the resonance is broad and the continuum level is changing, the width is somewhat difficult to characterize but, as described previously,[7] the resonance clearly extends into the bound portion of the spectrum. In 2-pentyne and 2- and 3-hexyne, the resonance is shifted somewhat to lower energy and is found to peak 0.4 - 0.5 eV above the corresponding

ionization energy. While these resonances are still broad, the resonance in 3-hexyne is significantly narrower than that in 2-butyne. Nevertheless, because the resonances in the larger alkynes are closer to threshold, the continuity of oscillator strength suggests that their influence on the bound-state spectrum is expected to be at least as important as in 2-butyne.[27,28]

The theoretical bond lengths for all of the C≡C triple bonds in the alkyne ground states investigated are very similar.[29] For example, the present calculations for 2-butyne and 3-hexyne indicate this bond length is only ~0.005 Å shorter in the former than in the latter; the C≡C bond length of 2-hexyne is between the 2-butyne and 3-hexyne values. Thus, the small shift of the resonance position in going from 2-butyne to 2-pentyne and 2- and 3-hexyne does not appear to result from a change in the C≡C bond length. This conclusion is consistent with previous results that suggest the position of π shape resonances is much less sensitive to bond length than is the position of σ shape resonances.[2]

Both 2-pentyne and 2-hexyne appear to show a second weaker, broad resonance lying approximately 0.75 eV above the first resonance that adds to the overall width of both features. This second resonance may result from the lower symmetry of these species as compared to 2-butyne and 3-hexyne. Note, however, that the splitting between the HOMO and HOMO-1 in these molecules is quite small (<0.1 eV), so that excitation from these two orbitals is unlikely to be the source of the two resonances. The second possibility is that the two resonances result from a similar splitting of the shape resonance. In particular, in 2-butyne, which has a quasi-linear backbone, the shape resonance has nominally $l = 4$, gπ symmetry, or e" symmetry in D_{3h}.[7] In the less symmetric molecules, this symmetry splits into resonances with A' and A" symmetry. Given the localization of the shape resonance on the linear four-carbon chain, this splitting is not expected to be large. However, the splitting might be expected to be somewhat larger than in the neutral ground state, because the relevant orbitals in the former have more nodes than in the latter, and the larger number of nodes may lead to larger energy changes as the molecule is

distorted. This possibility is discussed in more detail in Section III.b. With this explanation, however, a splitting is also expected for the shape resonance in 3-hexyne. It is possible that the weaker broad maximum observed at ~11.2 eV in Figure 6c corresponds to this second resonance.

For 1-butyne and the larger alkynes, there are also two or more stable conformers of the ground state neutrals that are populated at room temperature[30-35] and contribute to the absorption spectrum. However, these conformers differ in energy by less than 0.1 eV, and thus would not explain the significantly larger splittings between the resonances observed just above the ionization threshold. It also does not seem likely that the energy of the shape resonance will be strongly affected by the conformer. The four-carbon unit with the triple bond in the middle is relatively rigid, and the electron density in the HOMO and HOMO-1 of the neutral ground state is strongly localized on that four-carbon structure. The strong enhancement of absorption on resonance indicates that the final-state wavefunction is also localized in the same portion of the molecule. Thus, the electron density of the relevant orbitals is most likely small in the more flexible regions of the molecule away from the triple bond, and thus relatively independent of conformer. This feature also suggests that the observed behavior for terminal and internal alkynes should be quite general and relevant to both linear and branched alkynes, as well as to the corresponding radicals.

One possible alternative explanation for the resonances observed just above threshold is that they arise from autoionizing Rydberg states based on excited electronic states of the corresponding ion. According to the tables of Carlier et al.,[20] all of the larger alkyne cations except propyne and 2-butyne have excited electronic states within 1.3 to 2.5 eV of the lowest ionization thresholds. However, electronically autoionizing states converging to these thresholds would be expected for both the 1-alkynes and the 2- and 3-alkynes, and the observed absence of resonances in the 1-alkynes would be surprising, thus making this possibility unlikely. This explanation would also

not account for the very different ionization quantum yields determined for 1-butyne and 1-pentyne as compared to those of 2-butyne and 2-pentyne.

B. Theoretical Considerations

As a complement to the experimental results and discussion presented above, we have performed calculations of the continuum photoabsorption cross sections of the butynes, pentynes, and hexynes in the energy region just above the first ionization threshold. These calculations provide the partial cross sections as well, so that the contributions from the different l channels can be assessed. The calculations were performed as described previously for 2-butyne,[19,36-38] with the geometries fixed at the calculated equilibrium geometry of the corresponding neutral. The photoabsorption calculations were performed by using the ePolyScat codes[36,37] within the frozen-core Hartree-Fock approximation.[38] The transition moments were calculated in both the length and velocity gauges, and the length/velocity mixed gauge results are reported here.

Figure 7 shows the theoretical results for propyne, 1-butyne, 1-pentyne, and 1-hexyne. The partial cross sections represent the sum of contributions for excitation out of the HOMO and HOMO-1 of the initial state, but do not include contributions from more deeply bound orbitals. All four molecules show very similar behavior, as expected from the similar character of the HOMOs and (HOMO-1)s. In particular, the mixed p and d character of these orbitals and strong $l \rightarrow l + 1$ matrix elements result in large partial cross sections for the $l = 2$ and 3 partial waves. The $l = 3$ partial cross sections show only a weak energy dependence, but fall off at higher energy, while the $l = 2$ partial cross sections fall off much more rapidly with energy. The $l = 0$ and 1 partial cross sections are small for all three molecules, while the $l = 4$ cross section is small at threshold but rises gradually with increasing energy. The $l = 4$ behavior reflects the non-penetrating character of this partial wave at low energy.

The summed theoretical cross section for propyne rises slightly above threshold, then falls fairly rapidly with increasing energy. In contrast, the summed cross sections for the three larger 1-alkynes fall relatively fast just above threshold, and then more gradually with increasing energy. These theoretical results are reasonably consistent with the experimental results on propyne[17,39] and the larger 1-alkynes, but tend to fall off faster with increasing energy. This discrepancy may in part be due to the use of the fixed nuclei approximation in the calculations, and the corresponding neglect of vibrational motion. However, the magnitude of the theoretical total cross section is about a factor of two smaller than the experimental cross section. This observation will be discussed in more detail below.

Figure 8 shows the theoretical partial cross sections for 2-butyne, 2-pentyne, 2-hexyne, and 3-hexyne. A figure showing all of the theoretical partial cross sections for the alkynes in Figures 7 and 8 is included in the Supplemental Material.[25] In 2-butyne, the $l = 4$ partial wave dominates the cross section just above threshold as a result of an intense shape resonance in this channel.[19] However, although the theoretical $l = 4$ partial cross sections in the larger internal alkynes are substantial across the whole energy range (in contrast to the 1-alkynes), they do not show anything as dramatic as the enhancement shown for 2-butyne. The detailed behavior of the partial cross sections for other l values is also somewhat different, but the relative importance of the different partial waves is similar. In particular, the $l = 2$ and 3 partial cross sections are important throughout the energy range of the figure for all of the internal alkynes, while the $l = 0$ and 1 partial cross sections are of lesser importance. As in the case of the 1-alkynes, the magnitude of the theoretical total cross section is a factor of 2 - 3 smaller than the experimental cross section.

In the less symmetric alkyne systems, the l-dependent partial cross sections for the HOMO and HOMO-1 show the same overall trends, but differ somewhat from each other. In particular, although none of the cross sections show strong peaks, the positions of some of the maxima are

shifted by 1 - 2 eV in excitation from the HOMO relative to the HOMO-1. Thus, in principle, these differences could account for the splitting of the resonances discussed in Section III.a. The differences in the magnitudes of the HOMO and HOMO-1 partial cross sections are at most 2 - 3 Mb, however, which does not seem sufficient to account for the observed resonances in Figures 5 and 6. Separate partial cross sections for the HOMO and HOMO-1 and l = 2 - 4 are shown in the Supplemental Material.[25]

The importance of the l = 4 cross sections for the 2- and 3-alkynes, and the much smaller contribution of the l = 4 cross section to the 1-alkynes suggest that this partial wave is most likely responsible for the observed differences between the two sets of molecules, in agreement with the discussion above. Nevertheless, the question of the missing resonances in the calculations must be addressed. The shape resonances of interest correspond to π shape resonances, each with a nodal plane through the axis joining the four carbons on which the triple bond is centered. The calculation of the energy of these π resonances is known to be difficult because the energy is very sensitive to the nature of the molecular potential.[38] In the calculations presented here, the molecular potential has been modified to include correlation polarization, as has been described previously.[38] With this modification, the theoretical calculation effectively reproduces the 2-butyne experimental data.

Figure 9 shows a comparison of the l = 0 - 4 partial cross sections for ionization out of the HOMO alone obtained for 2-pentyne both with this correlation polarization and without it (i.e., standard Hartree-Fock). The latter shows a much larger cross section at threshold, particularly in the l = 3 and 4 channels. As discussed previously for 2-butyne, the l = 3 partial cross section likely gains its strength from coupling with the l = 4 channel, which carries the oscillator strength. Because the correlation polarization makes the potential more attractive, the large resonance appearing in the Hartree-Fock calculation would occur below the ionization threshold in the calculation with the modified potential. However, a large resonance below threshold

would be seen in the experimental photoabsorption data of Figure 5, and no obvious such resonance is observed. While the good agreement of the resonance position and intensity for 2-butyne provides some confidence in the magnitude of the correlation polarization correction to the potential in the larger systems, a number of other factors could affect the resonance position, including interchannel coupling and interactions with autoionizing states converging to electronically excited states of the ion. More detailed calculations on these larger molecules will be required to assess the relative importance of these effects, and to determine if the calculated resonance position can be shifted above threshold.

Finally, with the exception of 2-butyne and propyne, all of the theoretical photoabsorption cross sections are a factor of 2 to 3 smaller than the experimental cross sections. This observation is somewhat surprising given the good agreement for 2-butyne and propyne, and the expected accuracy (~±10%) of the experimental measurements. As seen in Figure 9, the details of the electron-ion potential can have a significant effect on the magnitude of the partial cross sections. However, the present discrepancy occurs both for the internal alkynes, where strong l = 4 resonances are expected, and for the 1-alkynes, where no l = 4 resonances are expected. One possibility is that the increased cross section comes from transitions to Rydberg series converging to excited electronic states of the alkyne cations. Excitation of these series corresponds to excitation out of initial state orbitals that are more strongly bound than the HOMO-1, and such excitations were not included in the present calculations. However, the excitation of these Rydberg series is generally expected to lead to observable series of resonances converging to the excited state thresholds, and no such series are observed in the experimental absorption spectra. It is possible that these resonances autoionize or predissociate extremely rapidly, but because there is no evidence for resonance features, the lifetimes must be very short. As discussed above, in 1-butyne, the quantum yield for ionization is only about 0.3 - 0.7 in the first 1.5 eV above threshold,[10,23] indicating that predissociation (or more specifically, radiationless transition followed by dissociation) is important, and no obvious resonance

structures are observed in the absorption spectrum.[23] Confirmation of this possibility in the other alkynes will require a detailed comparison of absolute photoabsorption and photoionization cross sections.

IV. CONCLUSION

Room-temperature absolute photoabsorption cross sections were recorded for the linear butynes, pentynes, and hexynes. The spectra of the terminal alkynes (1-butyne, 1-pentyne, and 1-hexyne) and the internal alkynes (2-butyne, 2-pentyne, and 2- and 3-hexyne) show very different behavior just above the first ionization threshold. In particular, all of the internal alkynes show a strong resonance within 1 eV of the threshold. The similarity of the structure of the HOMO and HOMO-1 in these internal alkynes suggests that these resonances have a common source, and the previous identification[7] of the resonance in 2-butyne as an $l = 4$, gπ shape resonance can be generalized to include all such internal alkynes. The observation of strong transitions from the ground state to high-l resonances occurs because, from the perspective of a single-center expansion, the ground state HOMOs in the internal alkynes have high-l character themselves. Because the corresponding shape resonances lie close to the ionization threshold, their influence is expected to extend into the bound portion of the spectrum, which should result in the observation of transitions from the ground state to $l = 4$ Rydberg series below threshold, as has recently been discussed for 2-butyne. Theoretical calculations support this analysis and the importance of the $l = 4$ channel in the photoabsorption of the 2- and 3-alkynes, but there are quantitative discrepancies between the experimental and theoretical spectra. Higher level calculations may be required to reproduce the details of the shape resonance structure. Because the resonant behavior is localized on the four-carbon unit containing the triple bond, similar behavior is also expected in branched alkynes. The alkynyl radicals should also display similar systematics. In particular, internal alkynyl radicals are expected to show a similar $l = 4$ shape resonance near the ionization threshold.

As discussed for 2-butyne in Section III, while the present conclusions reflect the results of photoabsorption measurements, they are also expected to have implications for the corresponding photoionization measurements and quantum yields. For larger molecules, radiationless transitions and predissociation often compete very effectively with autoionization, and even resonances undergoing fast electronic autoionization processes are weak due to competitive decay into these non-ionizing channels. However, the large widths for shape resonances (~0.5 eV - 1.0 eV for the alkynes presented here) suggest that ionization by tunneling through the barrier may be fast enough to compete effectively with these non-ionizing processes. The non-spherical nature of the molecular potential will also contribute to the large ionization width, as the barrier may exist along some escape directions but not others. Thus, overall, shape resonances are expected to enhance the photoabsorption signal and the ionization branching ratio. The results on 2-butyne and 2-pentyne[26] are consistent with this argument, while the absolute photoionization cross sections for the hexynes are currently unavailable.

ACKNOWLEDGEMENTS

We would like to thank Nils Hansen for providing data on the absolute photoionization cross sections of 1- and 2-pentyne prior to their publication. DMPH was supported by the Science and Technology Facilities Council, UK. This material is based on work supported by the U.S. Department of Energy, Office of Science, Office of Basic Energy Sciences, Division of Chemical Sciences, Geosciences, and Biosciences respectively under contract No. DE-AC02-06CH11357 (for HX and STP) and DE-SC0012198 (for RRL). RRL also acknowledges the support of the Robert A. Welch Foundation under grant A-1020. This work was supported by the Texas A&M University Supercomputing Facility. The experiments were performed on the DESIRS Beamline at SOLEIL under proposal numbers 20120675 and 20130934. We are grateful to the entire staff of SOLEIL for running the facility.

REFERENCES

1. Dehmer, J. L.; Parr, A. C.; and Southworth, S. H. Resonances in Molecular Photoionization. *Handbook on Synchrotron Radiation* **1987**, *2*, 241-353.
2. Stöhr, J. *NEXAFS Spectroscopy* (Springer, Heidelberg, 1996).
3. Piancastelli, M. N. The Neverending Story of Shape Resonances. *J. Electron Spectrosc. Rel. Phenom.* **1999**, *100*, 167-190.
4. Poliakoff, E. D.; Lucchese, R. R. Evolution of Photoelectron-Vibrational Coupling with Molecular Complexity. *Phys. Scripta* **2006**, *74*, C71-79.
5. Staniforth, M.; Daly, S.; Reid, K. L.; Powis, I. A Generic π^* Shape Resonance Observed in Energy-Dependent Photoelectron Angular Distributions from Two Colour, Resonant Multiphoton Ionization of Difluorobenzene Isomers. *J. Chem. Phys.* **2013**, *139*, 064304.
6. Bellm, S. M.; Davies, J. A.; Whiteside, P. T.; Guo, J.; Powis, I.; Reid, K. L. An Unusual π^* Shape Resonance in the Near-Threshold Photoionization of S_1 Para-Difluorobenzene. *J. Chem. Phys.* **2005**, *122*, 224306.
7. Xu, H.; Jacovella, U.; Ruscic, B.; Pratt, S. T.; Lucchese, R. R. Near-Threshold Shape Resonance in the Photoionization of 2-Butyne. *J. Chem. Phys.* **2012**, *136*, 154303.
8. Cool, T. A.; Nakajima, K.; Moustefaoui, T. A.; Qi, F.; McIlroy, A.; Westmoreland, P. R.; Law, M. E.; Poisson, L.; Peterka, D. S.; Ahmed, M. Selective Detection of Isomers with Photoionization Mass Spectrometry for Studies of Hydrocarbon Flame Chemistry. *J. Chem. Phys.* **2003**, *119*, 8356-8365.
9. Cool, T. A.; Wang, J.; Nakajima, K., Taatjes, C. A.; McIlroy, A. Photoionization Cross Sections for Reaction Intermediates in Hydrocarbon Combustion. *Int. J. Mass Spectrom.* **2005**, *247*, 18-27.
10. Wang, J.; Yang, B.; Cool, T. A.; Hansen, N.; Kasper, Near-Threshold Absolute Photoionization Cross Sections of Some Reaction Intermediates in Combustion. T. *Int. J. Mass Spectrom.* **2008**, *269*, 210-220.

11. Jorgensen, W. L.; Salem, L. *The Organic Chemist's Book of Orbitals* (Academic, New York, 1973).

12. Frisch, M. J.; Trucks, G. W.; Schlegel, H. B.; Scuseria, G. E.; Robb, M. A.; Cheeseman, J. R.; Scalmani, G.; Barone, V.; Mennucci, B.; Petersson, G. A.; Nakatsuji, H.; Caricato, M; Li, X.; Hratchian, H. P.; Izmaylov, A. F.; Bloino, J.; Zheng, G.; Sonnenberg, J. L.; Hada, M.; Ehara, M.; Toyota, K.; Fukuda, R.; Hasegawa, J.; Ishida, M.; Nakajima, T.; Honda, Y.; Kitao, O.; Nakai, H.; Vreven, T.; Montgomery, Jr., J. A.; Peralta, J. E.; Ogliaro, F.; Bearpark, M.; Heyd, J. J.; Brothers, E.; Kudin, K. N.; Staroverov, V. N.; Kobayashi, R.; Normand, J.; Raghavachari, K.; Rendell, A.; Burant, J. C.; Iyengar, S. S.; Tomasi, J.; Cossi, M.; Rega, N.; Millam, J. M.; Klene, M.; Knox, J. E.; Cross, J. B.; Bakken, V.; Adamo, C.; Jaramillo, J.; Gomperts, R.; Stratmann, R. E.; Yazyev, O.; Austin, A. J.; Cammi, R.; Pomelli, C.; Ochterski, J. W.; Martin, R. L.; Morokuma, K.;. Zakrzewski, V. G.; Voth, G. A.; Salvador, P.; Dannenberg, J. J.; Dapprich, S.; Daniels, A. D.; Farkas, Ö.; Foresman, J. B.; Ortiz, J. V.; Cioslowski, J.; Fox, D. J. Gaussian 09, Revision D.01, Gaussian, Inc., Wallingford CT, 2009.

13. Fano, U.; Cooper, J. W. Spectral Distribution of Atomic Oscillator Strengths. *Rev. Mod. Phys.* **1968**, 40, 441-507.

14. Slater, J. C. *Quantum Theory of Atomic Structure, Vol. I* (McGraw-Hill, New York, 1960).

15. de Oliveira, N.; Joyeux, D.; Phalippou, D.; Rodier, J.C.; Polack, F.; Vervloet, M.; Nahon, L. A Fourier Transform Spectrometer without a Beam Splitter for the Vacuum Ultraviolet Range: from the Optical Design to the First UV Spectrum. *Rev. Sci. Instrum.* **2009**, *80*, 043101.

16. de Oliveira, N.; Roudjane, M.; Joyeux, D.; Phalippou, D.; Rodier, J. C.; Nahon, L. Jigh-Resolution Broad-Bandwidth Fourier-Transform Absorption Spectroscopy in the VUV Range down to 40 nm. *Nat. Photonics* **2011**, *5*, 149 - 153.

17. Jacovella, U.; Holland, D. M. P.; Boyé-Péronne, S.; Joyeux, D.; Archer, L. E.; de Oliveira, N.; Nahon, L.; Lucchese, R. R.; Xu, H.; Pratt, S. T. High-Resolution Photoabsorption Spectrum of Jet-Cooled Propyne. *J. Chem. Phys.* **2014**, *141*, 114303.
18. A detailed discussion of potential sources of error in cross sections determined with the FTS will be presented in a forthcoming publication by N. de Oliveira, D. Joyeux, L. E. Archer, J. F. Gil, M. Roudjane, K. Ito and L. Nahon.
19. Jacovella, U.; Holland, D. M. P.; Boyé-Péronne, S.; Gans, B.; Joyeux, D.; Archer, L. E.; de Oliveira, N.; Nahon, L.; Lucchese, R. R.; Xu, H.; Pratt, S. T. High-Resolution Vacuum-Ultraviolet Photoabsorption Spectra of 1-Butyne and 2-Butyne. *J. Chem. Phys.* in press.
20. Carlier, P.; Dubois, J. E.; Masclet, P.; Mouvier, G. Spectres de Photoelectrons des Alcynes. *J. Electron Spectrosc. Rel. Phenom.* **1975**, *7*, 55-67.
21. Bieri, G.; Burger, F.; Heilbronner, E.; Maier, J. P. Valence Ionization Energies of Hydrocarbons. *Helv. Chim. Acta* **1977**, *60*, 2213-2233.
22. Jacovella, U.; Gans, B.; Merkt, F. Internal Rotation, Spin-Orbit Coupling, and Low-Frequency Vibrations in the $\tilde{X}^{+}\,^{2}$E Ground State of CH_3-CC-CH_3^+ and CD_3-CC-CD_3^+. *Mol. Phys.* doi:10.1080/00268976.2015.1005708 (in press).
23. Nakayama, T.; Watanabe, K. Absorption and Photoionization Coefficients of Acetylene, Propyne, and 1-Butyne. *J. Chem. Phys.* **1964**, *40*, 558-561.
24. Palmer, M. H.; Walker, I. C. The Electronic States of But-2-yne Studied by VUV Absorption, Near-Threshold Electron Energy Loss Spectroscopy, and Ab Initio Configuration Interaction Methods. *Chem. Phys.* **2007**, *340*, 158-170.
25. Supplemental Material.
26. Yang, B. and Hansen, N. private communication, 2015.
27. Allison, A. C.; Dalgarno, A. Continuity at the Dissociation Threshold in Molecular Absorption. *J. Chem. Phys.* **1971**, *55*, 4342-4344.

28. Smith, A. L. Continuity of Differential Oscillator Strength through a Dissociation Limit; Application to O_2 Schumann-Runge and Herzberg I Systems. *J. Chem. Phys.* **1971**, *55*, 4344-4350.

29. NIST Chemistry WebBook at http://webbook.nist.gov.

30. Holme, A.; Sæthre, L. J.; Børve, K. J.; Thomas, T. D. Carbon 1s Photoelectron Spectroscopy of 1-Pentyne Conformers. *J. Mol. Struct.* **2009**, *920*, 387-392, and references therein.

31. Bell, S.; Guirgis, G. A.; Li, Y.; and Durig, J. R. Far Infrared Spectrum, Ab Initio Calculations, and Conformational Analysis of 1-Pentyne. *J. Phys. Chem. A* **1997**, *101*, 5987-5996.

32. Utzat, K.; Bohn, R. K.; Michels, H. H. Four Conformers Observed and Characterized in 1-Hexyne, *J. Mol. Struct.* **2007**, *841*, 22-27.

33. Bell, S.; Guirgis, G. A.; Hur, S. W.; Durig, J. R. Infrared and Raman Spectra and Ab Initio Calculations for 2-Pentyne. *Spectrochim. Acta Part A* **1999**, *55*, 2361-2374.

34. Crowder, G. A.; Blankenship, P. Conformational and Vibrational Analysis of 2-Pentyne and 2-Hexyne, *J. Mol. Struct.* **1989**, *196*, 125-131.

35. Bohn, R. K. A Butane Analogue, 3-Hexyne, is Eclipsed. *J. Phys. Chem. A* **2004**, *108*, 6814-6816.

36. Gianturco, F. A.; Lucchese, R. R.; Sanna, N. Calculation of Low-Energy Elastic Cross Sections for Electron-CF_4 Scattering. *J. Chem. Phys.* **1994**, *100*, 6464-6471.

37. Natalense, A. P. P.; Lucchese, R. R. Cross Section and Asymmetry Parameter Calculation for Sulfur 1s Photoionization of SF_6. *J. Chem. Phys.* **1999**, *111*, 5344-5348.

38. Lucchese, R. R.; Raseev, G.; McKoy, V. Studies of Differential and Total Photoionization Cross Sections of Molecular Nitrogen. *Phys. Rev. A* **1982**, *25*, 2572-2587.

39. Ho, G. H.; Lin, M. S.; Wang, Y. L.; Chang, T. W. Photoabsorption and Photoionization of Propyne. *J. Chem. Phys.* **1998**, *109*, 5868-5879.

TABLE I. Ionization Energies, Resonance Positions, and C≡C Bond Lengths

Molecule	Ionization Energy (eV)[a]	Resonance Position (eV)[b]	2nd Resonance Position (eV)[b]	Ground State C≡C Bond Length (Å)[c]
Propyne	10.3674 ± 0.0001			1.2108
1-Butyne	10.178 ± 0.005			1.2141
2-Butyne	9.5611 ± 0.0006	10.415		1.2146
1-Pentyne	10.098 ± 0.005			1.2143
2-Pentyne	9.439 ± 0.005	9.857	10.464	1.2159
1-Hexyne	10.067 ± 0.005			1.2143
2-Hexyne	9.366 ± 0.005	9.795	10.539	1.2160
3-Hexyne	9.323 ± 0.005	9.832		1.2171

a. The ionization energy for propyne is from Xing *et al*. [*J. Chem. Phys.* **2008**, *128*, 094311]; that for 2-butyne is from Reference 22; all of the other ionization energies are from Reference 20.
b. The resonances are broad, and the positions represent the approximate centers of the features.
c. The bond lengths are from the present MP2 calculations with a 6-311++G (2df, p) basis set.

FIGURE CAPTIONS

Figure 1. The absolute photoionization cross sections for acetylene, propyne, and 1- and 2-butyne in the region of the first ionization threshold. The data for acetylene are from Reference 9. The data for propyne are from Reference 8, and the data for 1- and 2-butyne are from Reference 10.

Figure 2. (a) The highest occupied molecular orbital HOMO and HOMO-1 for the ground state of 1-butyne; (b) The two components of the HOMO for the ground state of 2-butyne. The energy difference between the corresponding HOMO and HOMO-1 is given by ΔE.

Figure 3. (a) - (b) The HOMO and HOMO-1 for 1- and 2-pentyne, and 1-, 2-, and 3-hexyne, respectively. The energy difference between the corresponding HOMO and HOMO-1 is given by ΔE.

Figure 4. The room-temperature, absolute photoabsorption cross sections of (a) 1-butyne and (b) 2-butyne recorded in this work. In part (a), the portion of the spectrum in blue is from the present work, while the portion in red is from the work of Nakayama and Watanabe.[23] The sharp lines marked by asterisks correspond to transitions in atomic impurities: Xe at 8.4365 eV, 9.5697 eV, and 10.4010 eV; O at 9.5214 eV; Kr at 10.0324 eV and 10.6436 eV; H at 10.1988 eV.[29]

Figure 5. The room-temperature, absolute photoabsorption cross sections of (a) 1-pentyne and (b) 2-pentyne recorded in the present work. The sharp line marked by an asterisk at 11.8281 eV corresponds to a transition in atomic Ar impurity.[29]

Figure 6. The room-temperature, absolute photoabsorption cross sections of (a) 1-hexyne, (b) 2-hexyne, and (c) 3-hexyne recorded in the present work. The sharp line marked by an asterisk at 11.8281 eV corresponds to a transition in atomic Ar impurity.[29]

Figure 7. Theoretical partial photoabsorption cross sections of propyne, 1-butyne, 1-pentyne, and 1-hexyne above the ionization threshold as a function of *l* and energy. The calculations only include excitation out of the HOMO and HOMO-1.

Figure 8. Theoretical partial photoabsorption cross sections of 2-butyne,[19] 2-pentyne and 2- and 3-hexyne above the ionization threshold as a function of *l* and energy. The calculations only include excitation out of the HOMO and HOMO-1.

Figure 9. Comparison of partial photoabsorption cross sections for ionization out of the HOMO of 2-pentyne obtained with and without correlation polarization (the latter labeled Hartree-Fock, or HF). (a) With correlation polarization; (b) without correlation polarization; (c) both calculations for the total cross section out of the HOMO.

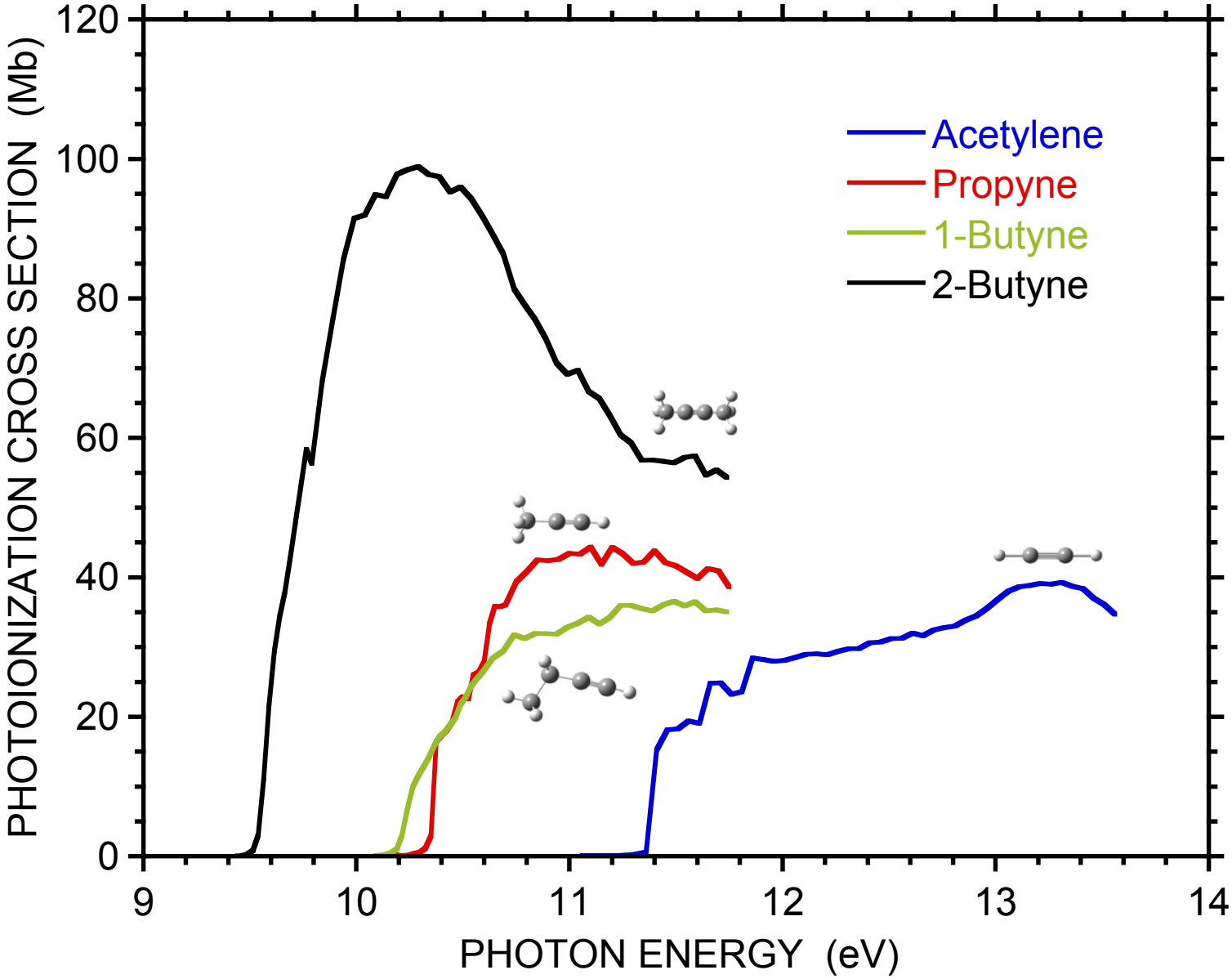
PHOTOIONIZATION CROSS SECTION (Mb)
120
100
80
60
40
20
0
9
10
11
12
13
14
PHOTON ENERGY (eV)
Acetylene
Propyne
1-Butyne
2-Butyne

Figure 1

1-Butyne

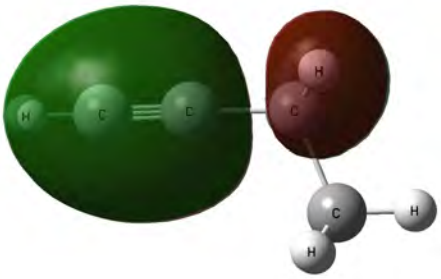

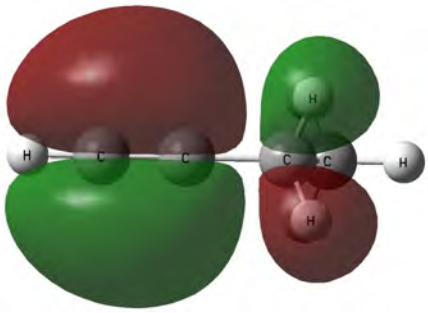

HOMO

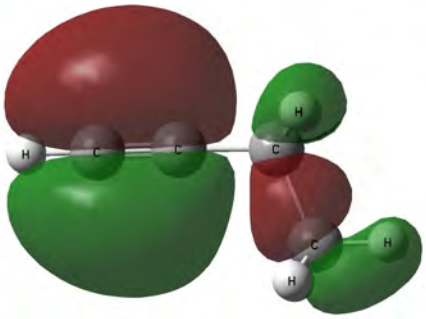

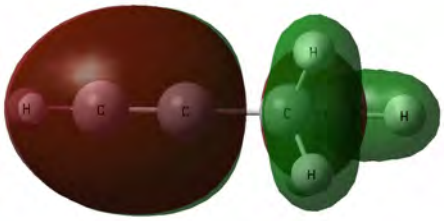

HOMO-1
(ΔE = -0.013 eV)

2-Butyne

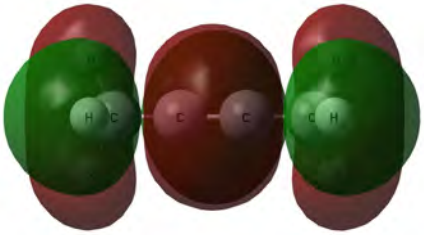

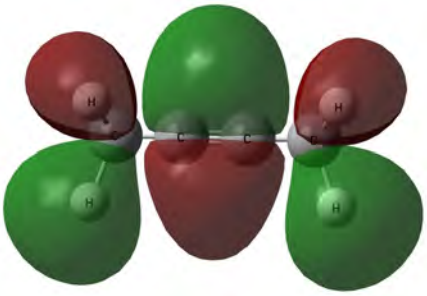

HOMO a

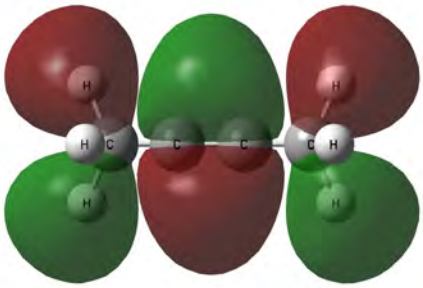

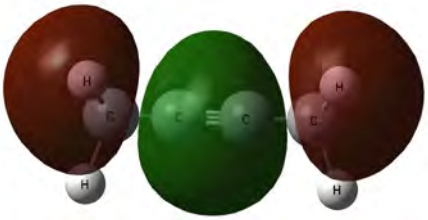

HOMO b

Figure 2

1-Pentyne

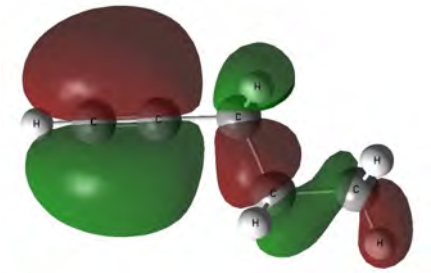

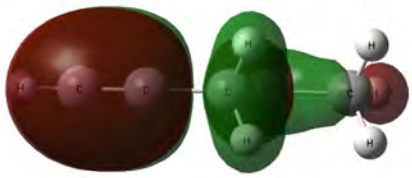

HOMO

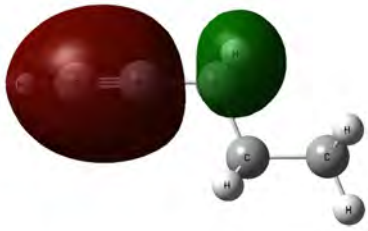

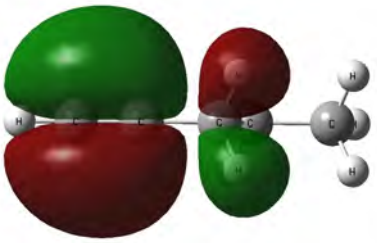

HOMO-1
(ΔE = -0.020 eV)

2-Pentyne

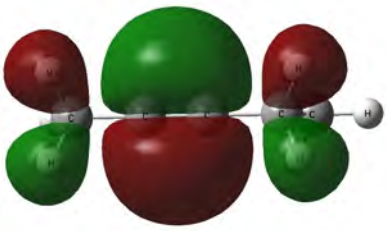

HOMO

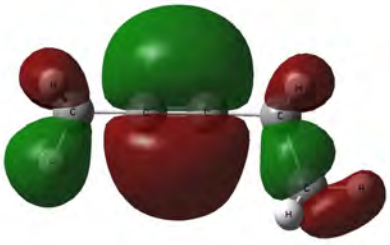

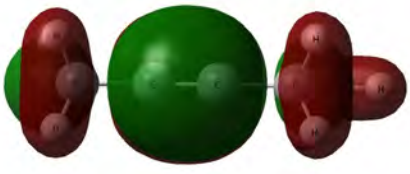

HOMO-1
(ΔE = -0.016 eV)

Figure 3a

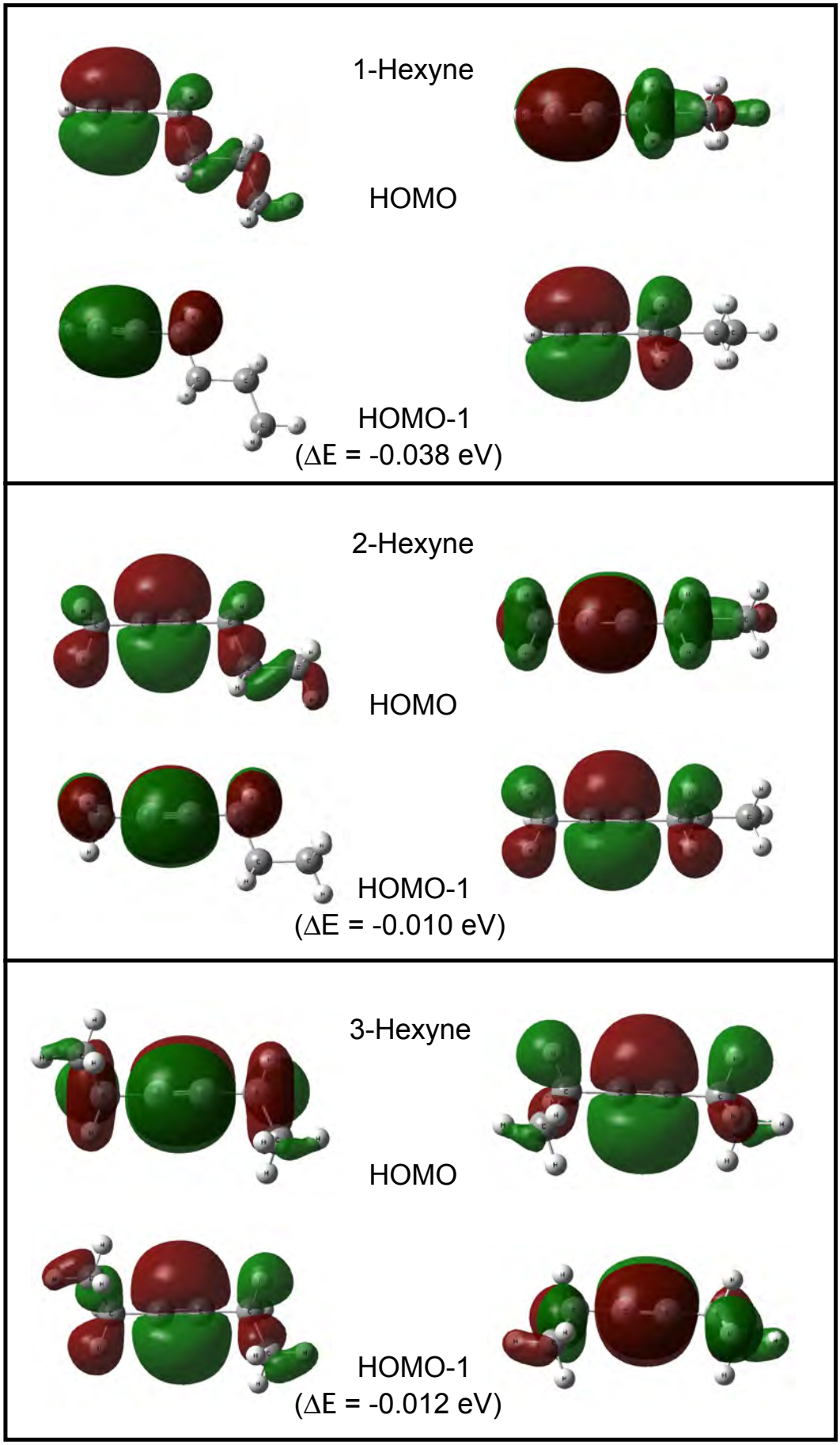
1-Hexyne
HOMO
HOMO-1
(ΔE = -0.038 eV)
2-Hexyne
HOMO
HOMO-1
(ΔE = -0.010 eV)
3-Hexyne
HOMO
HOMO-1
(ΔE = -0.012 eV)

Figure 3b

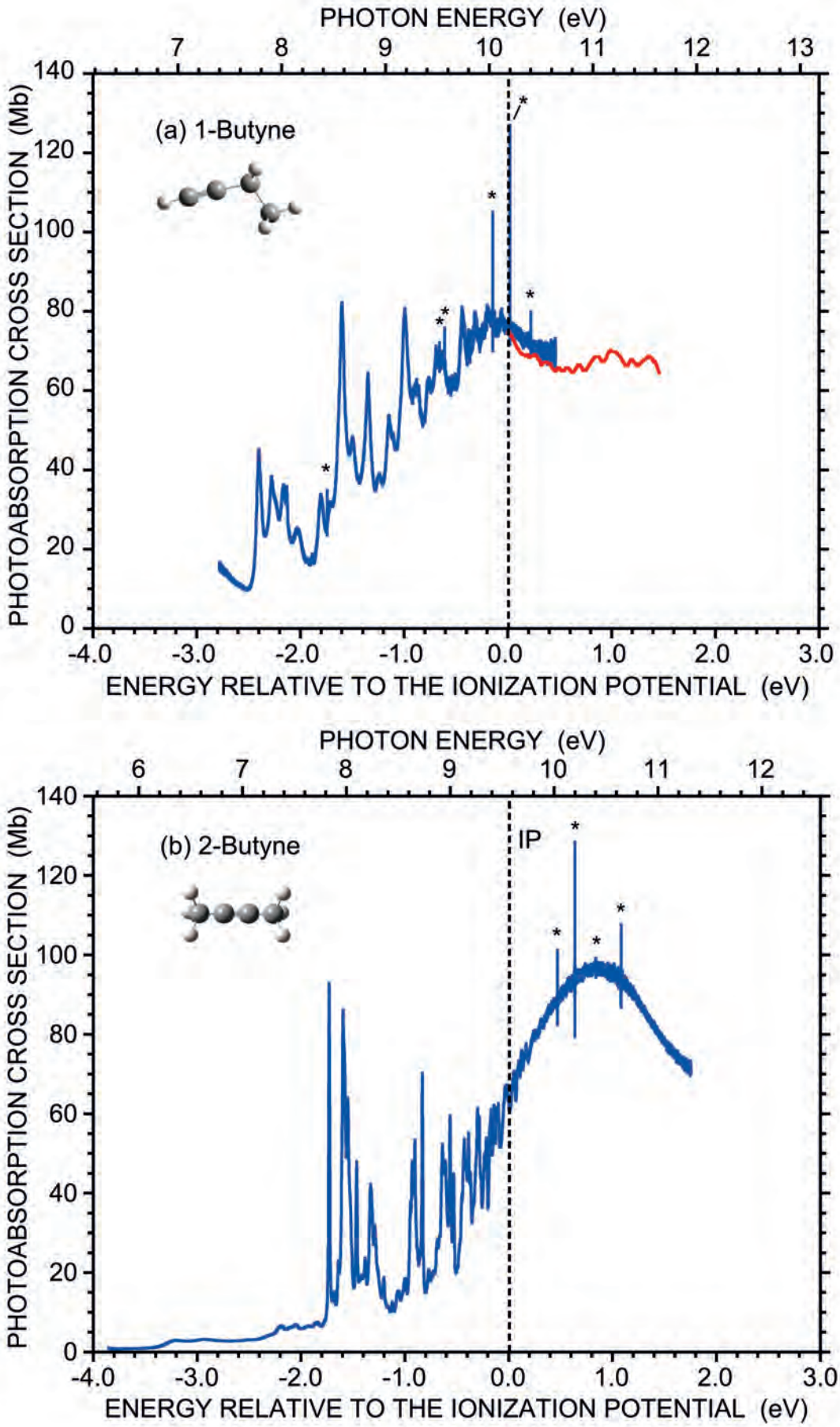
PHOTON ENERGY (eV)
7
8
9
10
11
12
13
140
120
100
80
60
40
20
0
PHOTOABSORPTION CROSS SECTION (Mb)
(a) 1-Butyne
*
*
*
*
*
-4.0
-3.0
-2.0
-1.0
0.0
1.0
2.0
3.0
ENERGY RELATIVE TO THE IONIZATION POTENTIAL (eV)
PHOTON ENERGY (eV)
6
7
8
9
10
11
12
140
120
100
80
60
40
20
0
PHOTOABSORPTION CROSS SECTION (Mb)
(b) 2-Butyne
IP
*
*
*
*
-4.0
-3.0
-2.0
-1.0
0.0
1.0
2.0
3.0
ENERGY RELATIVE TO THE IONIZATION POTENTIAL (eV)

Figure 4

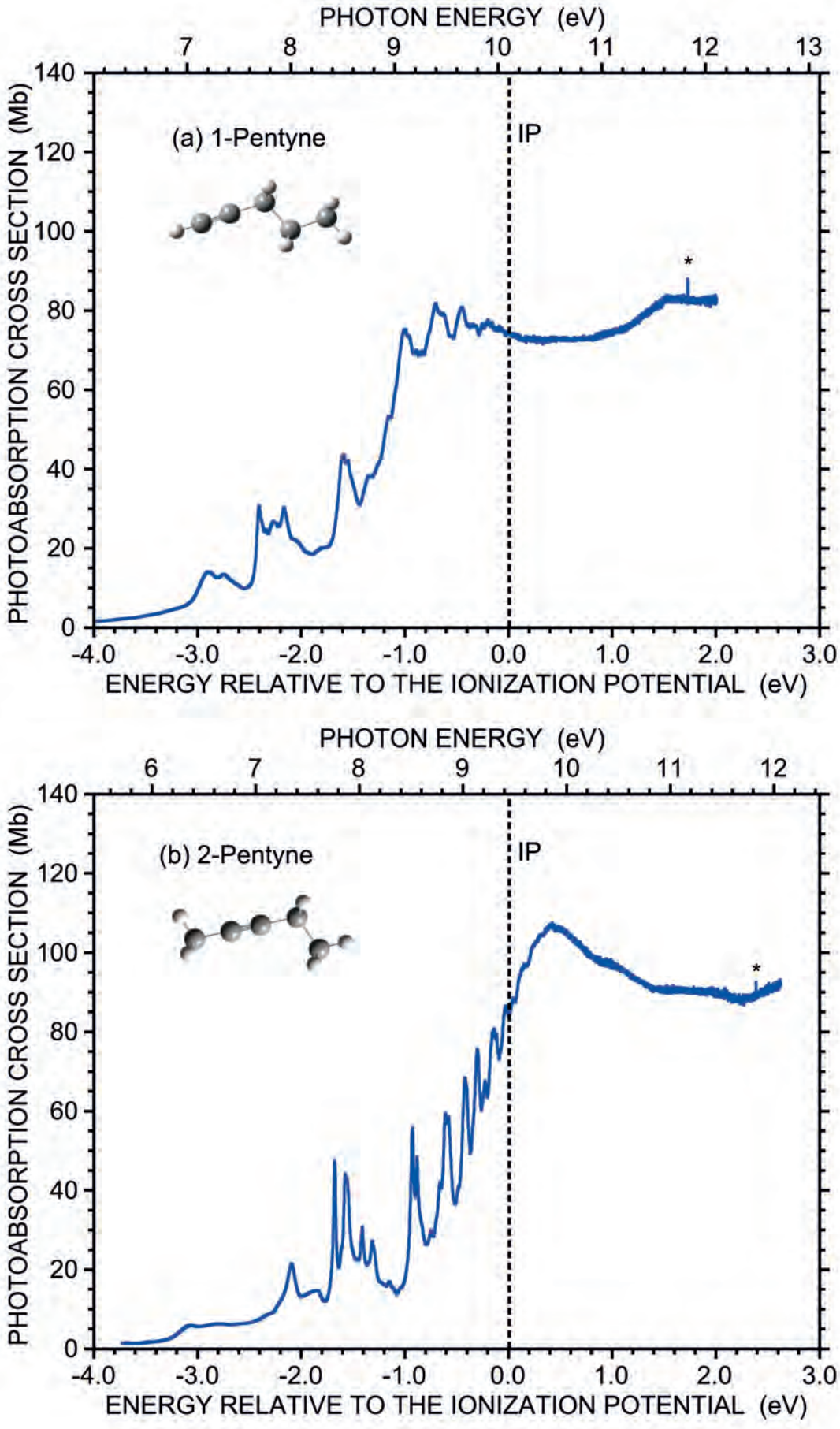
PHOTON ENERGY (eV)
7
8
9
10
11
12
13
140
120
100
80
60
40
20
0
PHOTOABSORPTION CROSS SECTION (Mb)
(a) 1-Pentyne
IP
*
-4.0
-3.0
-2.0
-1.0
0.0
1.0
2.0
3.0
ENERGY RELATIVE TO THE IONIZATION POTENTIAL (eV)
PHOTON ENERGY (eV)
6
7
8
9
10
11
12
140
120
100
80
60
40
20
0
PHOTOABSORPTION CROSS SECTION (Mb)
(b) 2-Pentyne
IP
*
-4.0
-3.0
-2.0
-1.0
0.0
1.0
2.0
3.0
ENERGY RELATIVE TO THE IONIZATION POTENTIAL (eV)

Figure 5

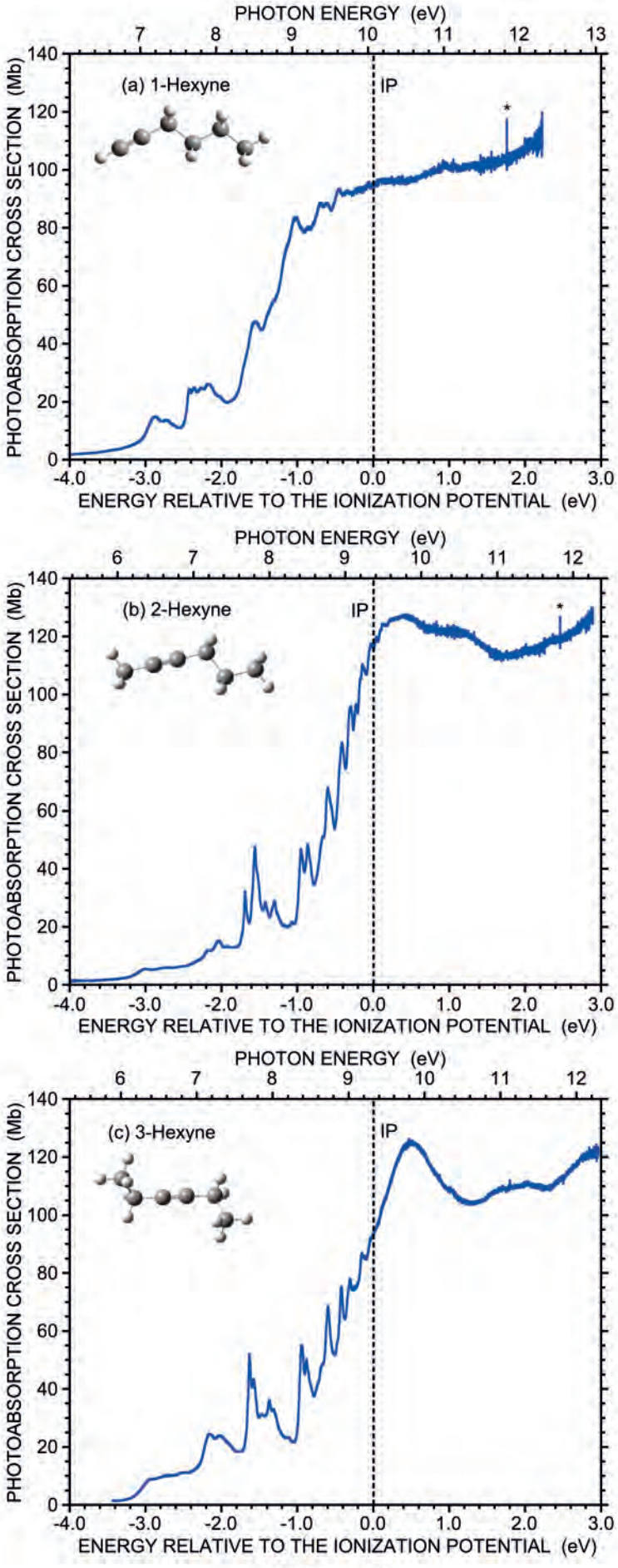
PHOTON ENERGY (eV)
7 8 9 10 11 12 13
(a) 1-Hexyne
IP
*
PHOTOABSORPTION CROSS SECTION (Mb)
0 20 40 60 80 100 120 140
-4.0 -3.0 -2.0 -1.0 0.0 1.0 2.0 3.0
ENERGY RELATIVE TO THE IONIZATION POTENTIAL (eV)
PHOTON ENERGY (eV)
6 7 8 9 10 11 12
(b) 2-Hexyne
IP
*
PHOTOABSORPTION CROSS SECTION (Mb)
0 20 40 60 80 100 120 140
-4.0 -3.0 -2.0 -1.0 0.0 1.0 2.0 3.0
ENERGY RELATIVE TO THE IONIZATION POTENTIAL (eV)
PHOTON ENERGY (eV)
6 7 8 9 10 11 12
(c) 3-Hexyne
IP
PHOTOABSORPTION CROSS SECTION (Mb)
0 20 40 60 80 100 120 140
-4.0 -3.0 -2.0 -1.0 0.0 1.0 2.0 3.0
ENERGY RELATIVE TO THE IONIZATION POTENTIAL (eV)

Figure 6

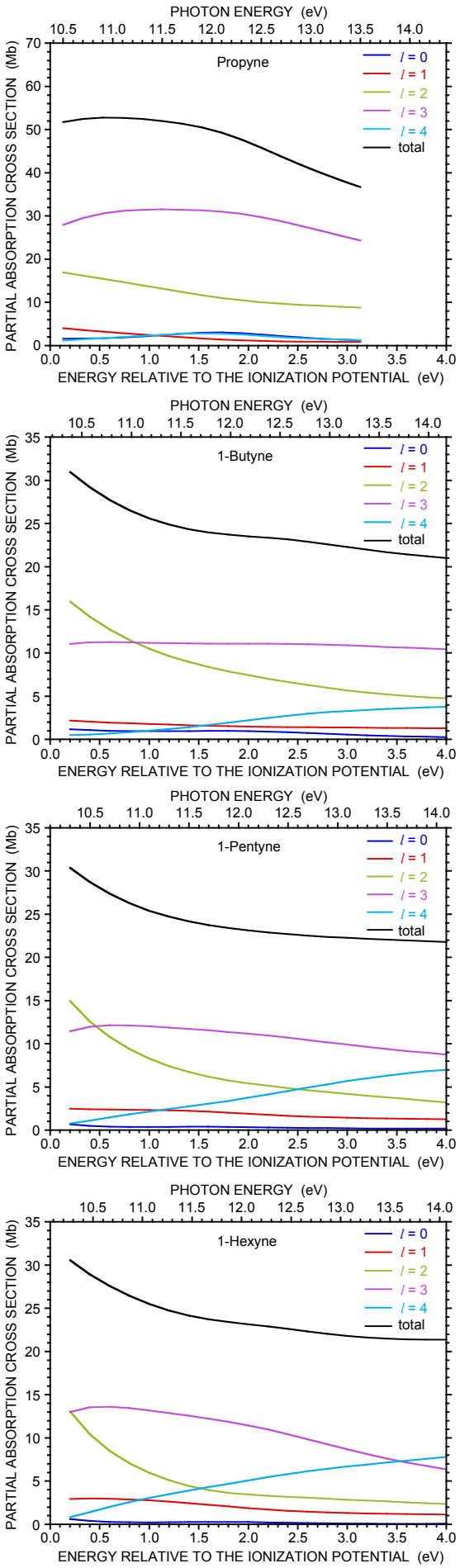
PHOTON ENERGY (eV)
10.5 11.0 11.5 12.0 12.5 13.0 13.5 14.0
Propyne
1-Butyne
1-Pentyne
1-Hexyne
l = 0
l = 1
l = 2
l = 3
l = 4
total
PARTIAL ABSORPTION CROSS SECTION (Mb)
ENERGY RELATIVE TO THE IONIZATION POTENTIAL (eV)
0.0 0.5 1.0 1.5 2.0 2.5 3.0 3.5 4.0

Figure 7

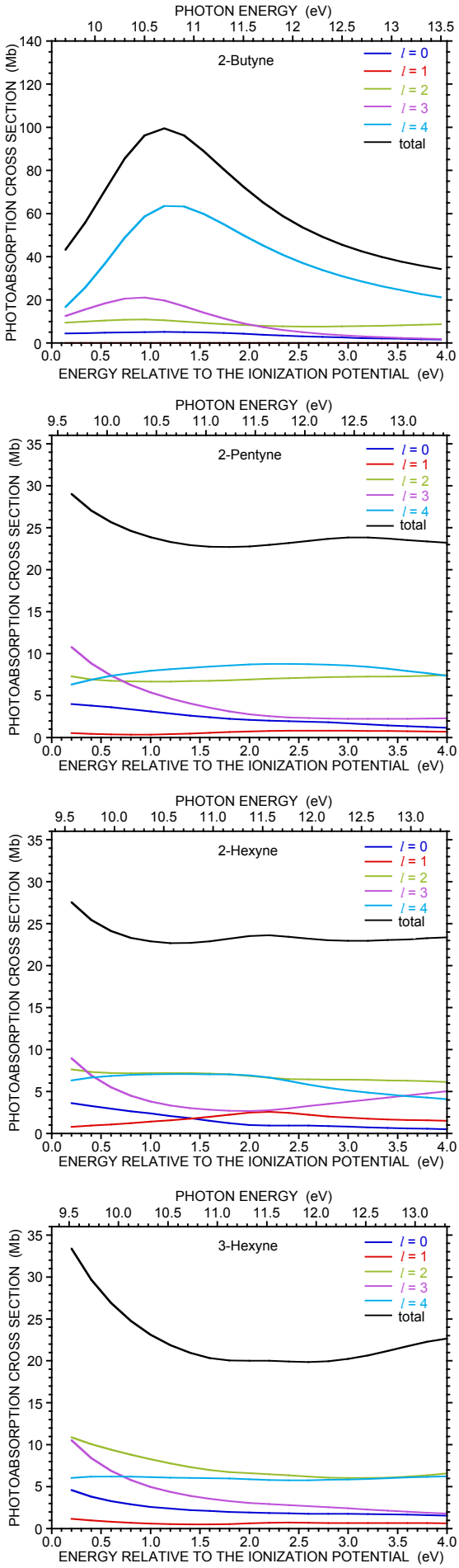
PHOTON ENERGY (eV)
2-Butyne
2-Pentyne
2-Hexyne
3-Hexyne
l = 0
l = 1
l = 2
l = 3
l = 4
total
PHOTOABSORPTION CROSS SECTION (Mb)
ENERGY RELATIVE TO THE IONIZATION POTENTIAL (eV)

Figure 8

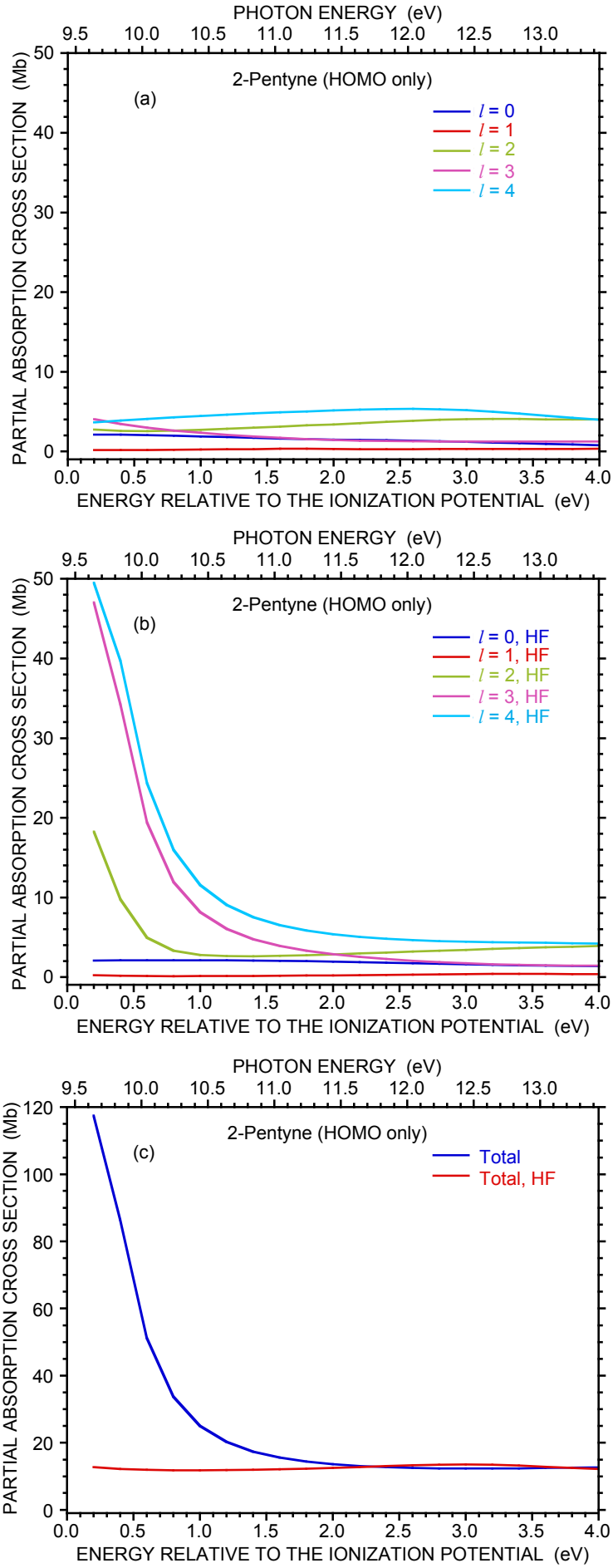
PHOTON ENERGY (eV)
9.5 10.0 10.5 11.0 11.5 12.0 12.5 13.0
2-Pentyne (HOMO only)
(a)
l = 0
l = 1
l = 2
l = 3
l = 4
PARTIAL ABSORPTION CROSS SECTION (Mb)
0 10 20 30 40 50
0.0 0.5 1.0 1.5 2.0 2.5 3.0 3.5 4.0
ENERGY RELATIVE TO THE IONIZATION POTENTIAL (eV)
PHOTON ENERGY (eV)
9.5 10.0 10.5 11.0 11.5 12.0 12.5 13.0
2-Pentyne (HOMO only)
(b)
l = 0, HF
l = 1, HF
l = 2, HF
l = 3, HF
l = 4, HF
PARTIAL ABSORPTION CROSS SECTION (Mb)
0 10 20 30 40 50
0.0 0.5 1.0 1.5 2.0 2.5 3.0 3.5 4.0
ENERGY RELATIVE TO THE IONIZATION POTENTIAL (eV)
PHOTON ENERGY (eV)
9.5 10.0 10.5 11.0 11.5 12.0 12.5 13.0
2-Pentyne (HOMO only)
(c)
Total
Total, HF
PARTIAL ABSORPTION CROSS SECTION (Mb)
0 20 40 60 80 100 120
0.0 0.5 1.0 1.5 2.0 2.5 3.0 3.5 4.0
ENERGY RELATIVE TO THE IONIZATION POTENTIAL (eV)

Figure 9